

LABORATORY INVESTIGATION

Cell rubidium uptake: A method for studying functional heterogeneity in the nephron

FRANZ X. BECK, ADOLF DÖRGE, ERNST BLÜMNER, GERHARD GIEBISCH, and KLAUS THURAU

Department of Physiology, University of Munich, Munich, Staticon, Planegg/Munich, Federal Republic of Germany and Department of Physiology, Yale University, School of Medicine, New Haven, USA

Cell rubidium uptake: A method for studying functional heterogeneity in the nephron. Rubidium uptake into individual tubule cells of rat renal cortex as measured by energy-dispersive X-ray microanalysis on freeze dried cryosections was used as an index of potassium transport. Over a 30 second period following intravenous infusion of rubidium (0.5 mmol/kg body wt) rubidium content increased in all cells. After 30 seconds, rubidium contents were (in mmol/kg dry wt): 225 ± 8 in distal convoluted tubule cells, 156 ± 7 in connecting tubule cells, 110 ± 7 in principal cells, 86 ± 4 in proximal tubule cells and 24 ± 2 in intercalated cells (mean \pm SEM). When distal sodium and potassium transport were stimulated by hypertonic saline loading, rubidium uptake was selectively increased into distal convoluted tubule cells by 38%, into connecting tubule cells by 36%, and into principal cells by 52%. However, rubidium uptake into proximal tubule and into intercalated cells remained unchanged. The preferential uptake of rubidium into distal convoluted tubule cells, connecting tubule cells, and principal cells correlates well with the known transport functions of sodium and potassium, whereas intercalated cells are distinguished by low sodium and potassium transport activity.

Experimental evidence supports the view that tubule segments beyond the macula densa play a key role in regulating renal sodium and potassium excretion. Although progress has been made in understanding the functions of these distal nephron segments, a direct assessment of ion transport in the individual cell types lining the distal tubule has been difficult. A major obstacle to the analysis of the cell mechanisms is the striking heterogeneity of this epithelium. The surface distal tubule comprises three, morphologically distinguishable segments: (1) the distal convoluted tubule, a segment composed exclusively of distal convoluted tubule cells; (2) the connecting tubule lined by connecting tubule and intercalated cells; and (3) the beginning portion of the cortical collecting duct, made up of principal and intercalated cells [1, 2]. The intermingling of different cell types within one tubular segment complicates the interpretation of studies of the transport properties of these nephron segments and of the different cell populations involved. There is now substantial evidence that principal cells mediate sodium absorption and potassium secretion [3]. Intercalated cells, however, are thought to be responsible for proton

and/or bicarbonate secretion and possibly for potassium absorption [3, 4].

Electron microprobe analysis of thin, freeze-dried cryosections with energy-dispersive X-ray detecting systems circumvents some of these difficulties, since this method allows for the simultaneous, quantitative determination of several electrolytes in individual, morphologically well-defined cells [5, 6]. Closely related by its physicochemical relationship to potassium, rubidium has often been used as marker for potassium, because rubidium often substitutes on K transport pathways [7–11]. In the present study we have employed a novel approach to monitor, by electron microprobe techniques, the time-dependent uptake of rubidium into individual cells of renal cortical tubules.

Thus, the determination of rubidium uptake into individual cells lining the distal convolution¹ as a function of time should provide information about cellular transport activities shared by rubidium with potassium. Furthermore, since potassium uptake in these cells is coupled to sodium exit via the $\text{Na}^+ - \text{K}^+ - \text{ATPase}$, changes in transcellular sodium movement should also be accompanied by alterations of rubidium transport. Therefore, rubidium uptake into renal tubule cells was measured in hydroponic control conditions and after an acute elevation of distal sodium delivery—a maneuver known to stimulate sodium absorption and potassium secretion along the surface distal tubule [12, 13]. Significant differences of rubidium movement were observed between the cells along this nephron, particularly that of principal and intercalated cells.

Methods

Preparation of animals and experimental protocol

The experiments were performed in two stages: First, renal clearance experiments were carried out to characterize overall

¹The term “distal convolution” is used to denote the following tubule segments: the distal convoluted tubule (distal convoluted tubule cells); the connecting tubule (connecting tubule and intercalated cells); and the beginning portion of the cortical collecting duct (principal and intercalated cells). The latter segment has also been termed the “initial collecting tubule.” The “early distal tubule” in micropuncture terminology comprises the distal convoluted tubule, the “late distal tubule” both connecting tubule and beginning portion of the cortical collecting duct [14, 15].

renal function. Secondly, rubidium was infused during well-defined periods after which the kidneys were excised for electron microprobe analysis.

Male Wistar rats (SAVO-Ivanovas, Kisslegg, FRG) were maintained on a standard rat diet (Altromin, Lage, FRG) and tap water until the day of study. Animals were anaesthetized by i.p. injection of inactin (Byk-Gulden, Konstanz, FRG; 100 to 120 mg/kg of body wt) and placed on a thermoregulated operating table to maintain body temperature at 37°C. After tracheotomy, catheters were inserted: (1) into the right jugular vein (infusion of isotonic saline, 5 ml/hr/kg body wt, and polyfructosan, 5 g/100 ml [Inutest, Laevosan-Gesellschaft, Linz, Austria]), (2) into the left femoral vein (injection of rubidium) and, (3) into the left femoral artery (to monitor blood pressure). The left kidney was exposed through a subcostal flank incision, freed of adherent fat and connective tissue and placed in a plastic cup. The exposed kidney was kept under a layer of paraffin oil, warmed to 38°C, to prevent cooling and desiccation. To allow timed urine collections, the renal pelvis was cannulated from the ureter with a polyethylene catheter. Blood samples were taken at the endpoints of each 25-minute collection period to determine plasma inulin concentrations.

At the end of the clearance periods the exposed kidney was rinsed several times with warm (38°C) Ringer's solution and rubidium chloride, either 0.33 (20 sec infusion) or 0.50 (30 sec infusion) mmol/kg body weight, administered as a continuous i.v. infusion. The kidney was removed from the animals after carefully timed intervals.

In a first set of experiments the following groups of animals were studied:

Group I ($N = 3$). Infusion of rubidium chloride over 20 seconds, removal of the kidney immediately at the end of the infusion period.

Group IIa ($N = 4$). Infusion of rubidium chloride over 30 seconds, removal of the kidney immediately at the end of the infusion.

Group IIb ($N = 3$). Duration of rubidium administration as in group IIa, but removal of the kidney 30 seconds after the end of the rubidium infusion.

Group IIc ($N = 3$). Duration of rubidium administration as in group IIa, but removal of the kidney seven minutes after the end of the rubidium infusion.

In an additional series of experiments ($N = 3$) rubidium chloride was given at a lower dose (0.13 mmol/kg body wt) over 30 seconds. Analyses of cell rubidium contents were done at only one time point, immediately following cessation of infusion.

Arterial blood for the determination of plasma rubidium concentration was obtained from the femoral artery during a 20 second period, the withdrawal being started 10 seconds before and terminated 10 seconds after excising the kidney. For shock-freezing, the whole kidney was plunged into a 1:3 (vol:vol) isopentane:propane mixture cooled to the temperature of liquid nitrogen.

In a second series of experiments an infusion solution containing 280 mM sodium chloride, 10 mM potassium chloride and 1 g/100 ml polyfructosan was administered at a rate of 25 ml/hr/kg body wt. The rationale of this experimental protocol was to increase distal sodium delivery and sodium absorption and potassium secretion along the surface distal tubule [12, 13].

In this series of experiments kidneys were obtained only at one time interval, immediately after terminating the 30-second rubidium infusion.

In some hydropenic animals ($N = 5$) FD+C green (100 μ l of a 1% solution) was injected via the femoral vein. The time which elapsed between the injection of the dye and its appearance in the capillary network of the renal cortex was 3.9 ± 0.1 seconds.

Tissue preparation for electron microprobe analysis and determination of cell rubidium and potassium contents

Small pieces of cortical tissue from the shock-frozen kidneys were mounted in a precooled ultracryomicrotome (modified Ultratome V, LKB, Bromma, Sweden) and 1 μ m thick cryosections cut at temperatures between -80 and -100°C . Sections were mounted between two thin films (formvar and collodion) and subsequently freeze-dried at -80°C and 10^{-6} torr. X-ray microanalysis of the freeze-dried cryosections was performed in a scanning electron microscope (S 150, Cambridge Instrument Ltd., Cambridge, UK) equipped with an energy-dispersive X-ray detecting system (Link Systems, High Wycombe, UK). The acceleration voltage was 20 kV and the probe current 0.3 nA. Small areas (1 to 2 μm^2) within the cells were scanned for 100 seconds and the emitted X-rays analyzed in the energy range between 0.2 and 20.0 keV. Further details about the preparation of freeze-dried cryosections for X-ray microanalysis have been described earlier [16].

The morphologic appearance of proximal tubule, distal convoluted tubule, principal and intercalated cells has also been described previously [6]. Proximal tubule cells were identified by a prominent brush border. The distal convoluted tubule could be recognized by its uniform cell type (the distal convoluted tubule cell) which, like proximal tubule cells, exhibited a comparatively dense cytoplasm, but no brush border. The cortical collecting duct showed two different cell types, light and dark appearing cells, that is, principal and intercalated cells. Cell height of both of them was somewhat less than in distal convoluted tubule cells. Cells of distal tubule origin with cytoplasmic electron density between that of distal convoluted tubule and principal cells and with similar cell height as distal convoluted tubule cells were designated as connecting tubule cells. Connecting tubule cells were observed only—as was the case for the principal cells—in tubular segments containing also intercalated cells.

Extra- and intracellular compartments in renal tubule cells are often intimately interdigitated (that is, basolateral infoldings, brush border). Hence, analyses of cytoplasmic areas completely free of extracellular spaces are difficult to obtain. Previous investigations, however, have clearly shown, firstly, that X-ray spectra obtained in the cell nuclei and in the cytoplasm adjacent to the nuclei reflect true cellular electrolyte concentrations not being modified by contributions originating from extracellular compartments and, secondly, that potassium concentrations are virtually identical in nucleus and cytoplasm [5, 6]. Consequently cellular measurements were in general confined to the nuclei. To confirm that the distribution of rubidium across the nuclear membrane is similar to that of potassium in the present experiments, additional electron probe analyses were also performed in both nucleus and perinuclear cytoplasm of selected tubule cells.

Table 1. Mean body weights, plasma electrolyte and clearance data

	Control	Hypertonic sodium chloride
Body weight g	180 ± 8	213 ± 20
Plasma potassium ^b mmol/liter	3.9 ± 0.1	3.7 ± 0.2
Plasma sodium mmol/liter	142.5 ± 0.8	150.3 ± 0.9 ^a
Urine flow rate μ l/min/100 g body wt	1.8 ± 0.2	27.2 ± 0.5 ^a
Glomerular filtration rate ml/min/100 g body wt	0.52 ± 0.02	0.53 ± 0.04
Urine potassium mmol/liter	292 ± 29	43 ± 7 ^a
Fractional potassium excretion %	25.0 ± 2.7	59.8 ± 9.5 ^a
Urine sodium mmol/liter	85 ± 20	273 ± 22 ^a
Fractional sodium excretion %	0.2 ± 0.1	9.2 ± 0.7 ^a
No. of animals	13	3

Values are means ± SEM

^a Significantly different from the corresponding control value

^b Plasma potassium concentrations obtained prior to rubidium injection

The separation of the X-ray continuum from the element-characteristic radiations was performed by a special computer program [17]. The cellular element concentrations were calculated in mmol/kg dry weight from the peak-continuum ratios, according to Hall [18].

Chemical analyses

The plasma and urine sodium and potassium concentrations were measured by flame photometry (Flame Photometer 543, IL, Lexington, Massachusetts, USA) and the plasma rubidium concentration by atomic absorption spectrophotometry (SP 9, Pye Unicam, Cambridge, UK). Urine osmolality was determined by the method of depression of vapor pressure (5100B, Wescor, Logan, Utah, USA). Inulin in plasma and urine was measured by the anthrone method of Führ, Kaczmarczyk and Krüttgen [19]. Standard formulae were used to calculate glomerular filtration rate and urinary excretion of sodium and potassium.

Presentation of data and statistical analysis

If not otherwise stated, the data are presented as means ± SEM with the number of measurements (*N*) in parentheses. Some of the differences between the means were tested for statistical significance using Student's *t*-test for unpaired data with *P* values less than 0.05 indicating significance. In addition, two-way analysis of variance was used to detect differences in rubidium contents between cell types in each group and differences in rubidium contents between different experimental groups for one cell type. The significance of differences between individual groups was further tested by *t*-test using appropriately adjusted significance levels [20]. Linear regression analysis was employed to assess initial uptake rates.

Results

Table 1 summarizes body weights, plasma electrolyte and clearance data under control conditions and following the administration of hypertonic sodium chloride. Plasma potassium concentrations and glomerular filtration rates were similar

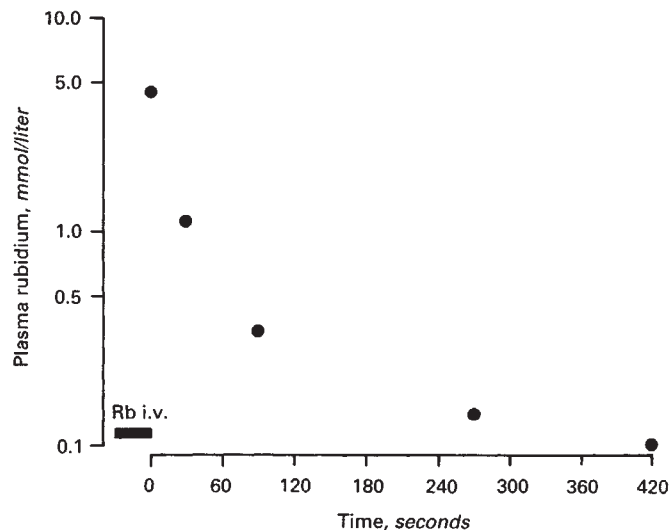


Fig. 1. Time course of arterial plasma rubidium concentration after a 30 second rubidium injection. Each point represents the mean of at least 3 single values. The ordinate is scaled logarithmically.

under both conditions. Infusing hypertonic saline led to a modest increase in the plasma sodium concentration and to a sharp rise in urine flow rate and sodium concentration, and in fractional sodium and potassium excretion. Urine potassium concentration, however, was markedly depressed in animals infused with hypertonic saline when compared with controls.

Figure 1 depicts the decline in plasma rubidium concentration after the injection of rubidium chloride over a time period of 30 seconds. Mean plasma rubidium was 4.48 mmol/liter at the end of the infusion period (group IIa) and had fallen to 1.07 mmol/liter 30 seconds after terminating rubidium administration (group IIb). The respective mean plasma potassium values were 4.8 ± 0.2 (*N* = 4) and 4.4 ± 0.1 (*N* = 3) mmol/liter. After 420 seconds the plasma potassium concentration was 4.2 ± 0.1 (*N* = 3) mmol/liter. The rapid initial decrease in plasma rubidium levels was followed by a slower decline so that after 120, 300 and 420 seconds, concentrations of 0.34, 0.14 and 0.10 mmol/liter were obtained. A similar time course of the rate of disappearance from plasma of rubidium [21] and potassium [22] has been observed using radioactive tracer techniques².

Following a rubidium injection lasting only 20 seconds (group I), plasma rubidium concentration was initially 4.72 mmol/liter, a value very similar to that observed in group IIa animals. These data show that during a well-defined, relatively short time period the present infusion protocol results in plasma rubidium concentrations comparable to those of normal plasma potassium levels.

Table 2 summarizes data on rubidium and potassium contents

² The rapidly changing plasma rubidium concentrations following the bolus injection reflect several processes, such as distribution into the extracellular fluid space, cell uptake and renal excretion. If rubidium were initially equally distributed in the extracellular fluid (about 25% of body weight), plasma rubidium concentrations should be between 2 and 3 mmol/liter. The observed values in excess of this (about 4.5 mmol/liter) indicate initially unequal distribution in the extracellular fluid. Later, further cell uptake and renal extraction and excretion reduce plasma rubidium concentrations to low levels.

Table 2. Rubidium and potassium contents obtained in nucleus and cytoplasm of proximal tubule cells

Group	<i>N</i>	mmol/kg dry wt		K/Rb	
		Rb	K	Rb	
I (20/0)	12	Nucleus	50.9 ± 7.1	599.3 ± 16.4	11.77
		Cytoplasm	31.9 ± 2.6	408.0 ± 14.9	12.79
IIa (30/0)	13	Nucleus	82.6 ± 6.2	546.1 ± 20.4	6.61
		Cytoplasm	59.5 ± 5.7	404.0 ± 23.2	6.79
IIb (30/30)	16	Nucleus	117.3 ± 3.0	484.9 ± 12.2	4.13
		Cytoplasm	88.8 ± 4.5	383.8 ± 13.0	4.32
IIc (30/420)	21	Nucleus	77.4 ± 2.6	503.1 ± 17.5	6.50
		Cytoplasm	64.4 ± 2.4	376.0 ± 15.5	5.84

Values are means ± SEM; *N* indicates number of cells. All cytosolic rubidium and potassium contents are significantly lower than the corresponding values in the nucleus. For corrections due to differences in dry weight between nucleus and cytoplasm see text. The duration of the rubidium infusion and the time interval between terminating the infusion and shock-freezing the kidney are given in parentheses (in sec). K/Rb is the ratio of potassium to rubidium content for either nucleus or cytoplasm

measured in the nucleus of proximal tubule cells. These are compared with similar values in cytoplasmic regions of the same cells. It is apparent that within each group of animals the ratios of rubidium to potassium for nucleus and cytoplasm were similar. This observation supports the view that in both cell compartments rubidium is freely exchanging with potassium. Similar observations were also obtained in distal convoluted tubule cells of group I and group IIa animals, experimental conditions in which the time to rubidium exposure was very brief. The potassium to rubidium ratio was 3.6 and 4.2 for nucleus and cytoplasm in group I (*N* = 8), and 2.2 and 2.5, respectively, in group IIa (*N* = 7). Hence, the distribution of rubidium between nucleus and cytoplasm in these cells is also not markedly different from that of potassium. Inspection of Table 2 also shows that the contents of potassium and rubidium (expressed as mmol/kg dry weight) in proximal convoluted tubule cells were consistently higher in the nucleus than in the cytoplasm. However, since previous studies have shown that the dry weight of the cytoplasmic region is higher than that of the nucleus [5, 6], the present data are consistent with the conclusion that the concentrations of potassium and rubidium are similar in the nucleus and cytoplasm³.

Figure 2 shows energy-dispersive X-ray spectra in intercalated and distal convoluted tubule cells, either not exposed to rubidium or subjected to a 30 second rubidium exposure. It is evident that rubidium is taken up much faster by distal convoluted tubule cells than by intercalated cells. The uptake of rubidium into distal convoluted tubule cells is paralleled by a marked decline in the intensity of the potassium signal.

Table 3 summarizes data on rubidium and potassium contents in individual tubule cells after either a 20 or 30 second rubidium injection (group I and IIa animals), or after a longer exposure time, of 30 or 420 seconds, respectively, following rubidium administration for 30 seconds (group IIb and IIc animals). Several points deserve comment. Infusing rubidium intravenously for 30 seconds leads to an increase in rubidium content of all tubule cell types analyzed when compared to the rubidium uptake following a 20 second infusion. If the rise in cell

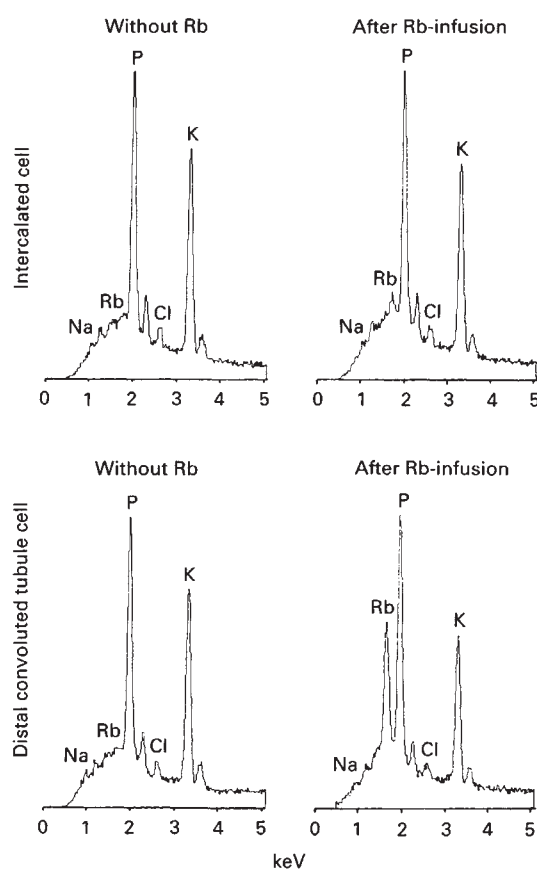


Fig. 2. Energy-dispersive X-ray spectra obtained in intercalated and distal convoluted tubule cells. Spectra were taken in cells not exposed to rubidium, and immediately after a 30 sec rubidium injection (group IIa).

rubidium content is assumed to be linear during a 30 second infusion period, as depicted in Figure 3A, the intersections of the individual regression lines with the abscissa scatter around a mean value of 6 seconds (minimum 2 sec: principal cells; maximum 9 sec: intercalated cells). This time interval is in reasonable agreement with the transit time (4 sec) obtained for the passage of FD+C green between left femoral vein and renal

³ The mean dry weight of the nucleus is 23 g%, that of the cytoplasm 32 g% [5, 6]. Accordingly, the derived concentrations of both potassium and rubidium in nucleus and cytoplasm are almost identical.

Table 3. Rubidium and potassium contents of renal tubule cells exposed for different time intervals to rubidium

	Group	N	Rb	K
			mmol/kg dry weight	
Proximal tubule cells	I (20/0)	38	50.1 ± 3.0	571.3 ± 9.2
	IIa (30/0)	36	86.0 ± 4.4	564.6 ± 13.3
	IIb (30/30)	35	118.0 ± 3.2	472.2 ± 10.4
	IIc (30/420)	27	80.4 ± 2.4	524.1 ± 16.9
Distal convoluted tubule cells	I (20/0)	48	132.5 ± 6.3	478.3 ± 14.4
	IIa (30/0)	53	224.9 ± 8.4	436.6 ± 12.4
	IIb (30/30)	47	190.0 ± 4.0	433.0 ± 10.6
	IIc (30/420)	51	51.7 ± 1.1	565.1 ± 13.5
Connecting tubule cells	I (20/0)	33	85.5 ± 3.6	599.4 ± 13.3
	IIa (30/0)	42	156.1 ± 6.7	535.5 ± 16.1
	IIb (30/30)	26	168.2 ± 6.4	477.0 ± 17.7
	IIc (30/420)	26	56.1 ± 1.7	613.2 ± 20.5
Principal cells	I (20/0)	38	71.2 ± 4.4	647.7 ± 13.6
	IIa (30/0)	36	109.7 ± 6.9	630.9 ± 15.7
	IIb (30/30)	33	141.3 ± 5.7	552.8 ± 11.0
	IIc (30/420)	34	53.0 ± 1.5	671.1 ± 15.9
Intercalated cells	I (20/0)	37	12.5 ± 0.9	591.8 ± 15.8
	IIa (30/0)	42	23.7 ± 1.6	627.6 ± 16.5
	IIb (30/30)	35	26.4 ± 0.9	565.3 ± 15.2
	IIc (30/420)	34	41.7 ± 1.9	594.9 ± 17.7

Values are means ± SEM; N indicates number of cells. The duration of the rubidium infusion and the time interval between terminating the infusion and shock-freezing the kidney are given in parentheses (in sec). Statistic evaluation of differences by two-way analysis of variance indicates differences between individual cells for each time interval as well as differences in one specific cell type at different time intervals. For specific information see Table 4.

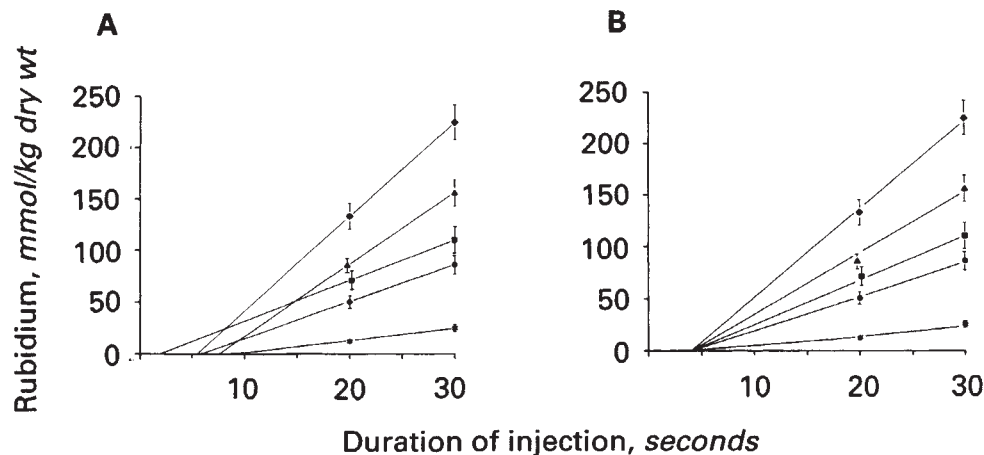


Fig. 3. Rubidium contents in tubule cells observed immediately at the end of either a 20 (group I) or 30 second (group IIa) rubidium infusion. The data are given as mean ± 2 SEM. **A.** Data of individual experimental groups were used to calculate linear regression lines. **B.** Linear regression lines of individual experimental groups calculated with the assumption of a 4 sec appearance time of rubidium in the renal cortex. Analysis of variance of regression coefficients indicates significant difference between the slopes of the regression lines ($P < 0.0001$). Symbols are: (◆) distal convoluted tubule cell; (▲) connecting tubule cell; (■) principal cell; (●) proximal tubule cell; and (*) intercalated cell.

capillary network. Hence, it is reasonable to conclude that after the time at which rubidium has reached the renal cortex (4 sec after the begin of infusion) rubidium uptake is linear for another 26 seconds. This indicates that during this time cell rubidium contents are not significantly affected by rubidium efflux from cell to extracellular spaces, and that the rubidium uptake data obtained immediately after either a 20 or 30 second rubidium injection represent an estimate of unidirectional rubidium influx from extracellular fluid into the cytoplasm.

Inspection of Figure 3 B shows that rubidium uptake was fastest in distal convoluted tubule cells and slowest in interca-

lated cells. In proximal tubule cells rubidium uptake was less rapid than in either connecting tubule or principal cells. In this graph initial uptake rates of rubidium were estimated by linear regression analysis assuming that the injected rubidium reaches the renal cortex after 4 seconds. The following uptake rates were calculated (mmol/kg dry wt/sec): distal convoluted tubule cells: 8.6, connecting tubule cells: 5.9, principal cells: 4.3, proximal tubule cells: 3.3, and intercalated cells: 0.9.

Table 4 summarizes differences of rubidium uptake after two time intervals following 30 second injections (groups IIa and IIc). In the upper right hand section of the Table, the differences

Table 4. Summary of statistical data of rubidium uptake

	Proximal tubule cells	Distal convoluted tubule cells	Connecting tubule cells	Principal cells	Intercalated cells
Proximal tubule cells	—	$P < 0.001$	$P < 0.001$	$P < 0.05$	$P < 0.001$
Distal convoluted tubule cells	$P < 0.001$	—	$P < 0.001$	$P < 0.001$	$P < 0.001$
Connecting tubule cells	$P < 0.001$	$P = \text{NS}$	—	$P < 0.001$	$P < 0.001$
Principal cells	$P < 0.001$	$P = \text{NS}$	$P = \text{NS}$	—	$P < 0.001$
Intercalated cells	$P < 0.001$	$P < 0.001$	$P < 0.001$	$P < 0.001$	—

Upper right section compares data of group IIa, lower left section data of group IIc. The comparison was performed by *t*-tests using Bonferroni's correction of significance levels.

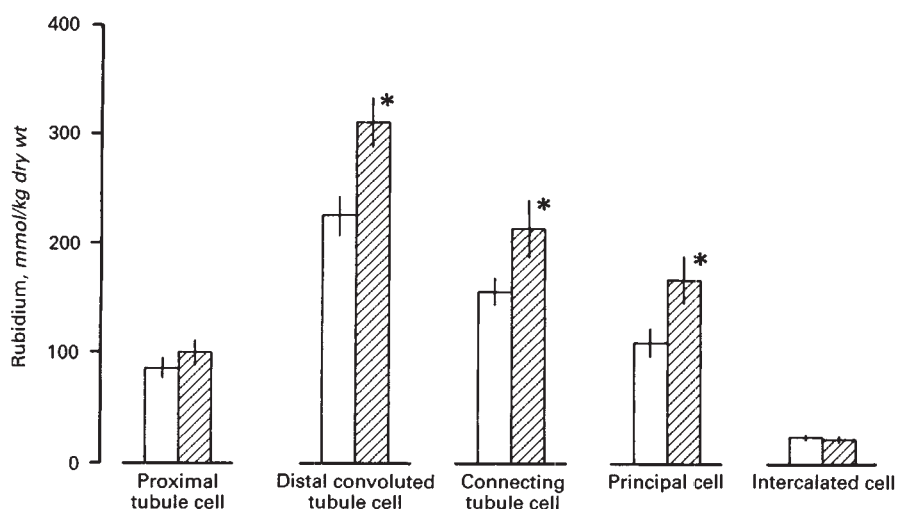


Fig. 4. Rubidium contents in tubule cells obtained immediately at the end of a 30 second rubidium administration in controls (clear bars) and following infusion of hypertonic saline (striped bars). The data are given as mean \pm 2 SEM.

of rubidium contents between individual tubule cells of group IIa are summarized. The differences of rubidium contents between all cell types are statistically significant. As pointed out above, these data support the view of heterogeneity of uptake mechanisms in different tubule cells.

Attention should be focused on the observation that after terminating the rubidium infusion, plasma rubidium concentrations exhibited a fast decline (Fig. 1). A parallel reduction in cellular rubidium could be observed only in distal convoluted tubule cells, where the rubidium content had decreased significantly during the 30 seconds following the rubidium injection. In contrast, in connecting tubule and intercalated cells, rubidium content remained stable, it even further increased in proximal tubule and principal cells.

In group IIc animals (420 sec after the injection period) rubidium content in distal convoluted tubule, connecting tubule, principal and intercalated cells were of comparable magnitude, while that of proximal tubule cells was clearly highest at this time. This observation indicates that during the rapid fall in plasma rubidium concentrations rubidium efflux from cell to the extracellular compartment is slower in proximal tubule cells than in distal convoluted tubule, connecting tubule and principal cells. The same may be true for intercalated cells, where despite the sharp fall in extracellular rubidium concentration over the 420 second period, even a modest rise in cell rubidium content was observed.

In Table 4 (lower left section) are also included statistical analyses of the differences of rubidium contents between individual cells after 420 seconds (group IIc). While proximal tubule cells had higher rubidium contents than all other cells, rubidium content of intercalated cells was significantly lower than that of all other cells investigated.

Hypertonic sodium chloride was infused at a rate known to increase both sodium concentration and flow rate of distal tubule fluid, to study the effect of an increase in sodium absorption and potassium secretion along the distal tubule on cell rubidium uptake. The data obtained at the end of a 30 second rubidium injection are depicted in Figure 4. Compared with controls, rubidium content was higher by 86.4, 56.4 and 57.1 mmol/kg dry wt, in distal convoluted tubule, connecting tubule and principal cells, respectively. No major alterations in cell rubidium levels, however, were observed in proximal tubule and intercalated cells. Hence, the increase in distal sodium delivery was accompanied by a sharp rise in rubidium uptake of only those cells known to be activated, and to mediate and sustain enhanced levels of transepithelial sodium and potassium transport.

Discussion

Critique of the method

In the present study we have used rubidium as a probe for studying the transport pathways of potassium in individual

renal tubule cells. Due to the close physicochemical relationship of the two group I alkali metal ions, rubidium has often been used as a physiological marker ion for potassium. Experimental evidence supporting the validity of this use of rubidium has been obtained, firstly, from renal clearance experiments showing that under a variety of experimental conditions rubidium and potassium are handled similarly by the kidney [8, 10] and, secondly, from the results of perfusion experiments in isolated tubule segments in vitro, demonstrating comparable transepithelial tracer fluxes of both rubidium and potassium [23], as well as similar responses of potassium and rubidium fluxes to well defined modulators of potassium transport [11, 24]. Despite these observations, differences between the transport patterns of potassium and rubidium should also be noted [10, 25].

In preliminary experiments we injected a bolus of rubidium chloride into the abdominal aorta above the renal arteries to achieve high rubidium concentrations in the plasma entering the renal artery, and to minimize the time delay between the start of the injection and the time of arrival of rubidium at renal tubule cells. Although in these experiments we observed marked differences in rubidium uptake between various tubule cell types, these data showed a wide scatter. This was probably due to the effects of high, local plasma rubidium concentrations on renal hemodynamics, as evidenced by blanching of surface patches of the renal cortex. Infusing rubidium intravenously via the femoral vein circumvented this difficulty. This approach, however, leads to prolongation of the time lag between onset of injection and appearance of rubidium in the renal circulation. However, we have chosen the intravenous route of rubidium administration because of the satisfactory reproducibility of cell uptake data and because of the absence of adverse renal hemodynamic effects.

Both methods of administering rubidium in vivo preclude attainment of stable plasma rubidium concentrations for longer time intervals so that constant extracellular conditions for rubidium uptake by tubule cells are not provided. In addition, the analytical constraints of the method prevent the use of rubidium in tracer doses so that competition between rubidium and potassium on cell transport pathways cannot be avoided. Such competition could account for the reduction in cell potassium content observed during rubidium administration. It should be noted that following the administration of smaller doses of rubidium (0.13 mmol/kg body wt) a similar pattern of differential rubidium uptake was observed. The following rubidium contents were obtained (mmol/kg dry wt): proximal convoluted tubule cell ($N = 29$), 33.2 ± 1.3 ; distal convoluted tubule cell ($N = 33$), 64.4 ± 4.7 ; connecting tubule cell ($N = 20$), 46.5 ± 3.0 ; principal cell ($N = 29$), 38.1 ± 2.1 , and intercalated cell ($N = 30$), 10.3 ± 0.8 . However, in most of the present experiments a higher dose of rubidium was chosen to assure accurate distinction of differential cell uptake into individual tubule cells as well as adequate monitoring of the time course of rubidium levels in tubule cells and plasma.

Routes of cell rubidium uptake

The rubidium contents of renal tubule cells obtained by electron microprobe analysis do not allow precise discrimination between the individual flux components into and out of tubule cells. Rather, they represent the result of net cell

rubidium uptake. However, a reasonable estimate of unidirectional rubidium influx from the extracellular fluid into the cytoplasm is provided by measurements of cell rubidium contents performed very shortly after administering this marker ion. In the present study, a minimum of 20 seconds elapsed between the onset of the intravenous rubidium infusion and the removal of the kidney for analysis. Since another 4 seconds elapsed from the beginning of the injection until rubidium ions reached the renal tubule cells (FD+C dye transit time data in **Methods**), the shortest exposure of the tubule epithelium was some 16 seconds. Since rubidium in all cell types increased linearly with time for a period of 30 seconds, the uptake data obtained over either 20 or 30 seconds should provide a reasonable estimate of unidirectional rubidium influx.

Rubidium may enter tubule cells by at least one of these different transport modes: 1) actively via the $\text{Na}^+ - \text{K}^+ - \text{ATPase}$. Experiments in several tissues have provided firm evidence that rubidium is handled by this enzyme very similarly to potassium [26]; 2) by secondary active transport via potassium-accepting carriers molecules that mediate $\text{Na}/2\text{Cl}/\text{K}$ cotransport or K/Cl cotransport [27, 28, Dörge A., Rick R., Beck F, Thureau K., unpublished observations]. There is evidence suggesting that rubidium can use both of the above mentioned cotransporters. 3) In addition, rubidium ions may be moving passively by electrodiffusion via potassium-selective ion channels. Studies on various epithelial tissues, however, support the notion that some potassium-selective channels do not permit unrestricted passage of rubidium [29, 30].

The present results on rubidium uptake into renal tubule cells do not allow to discriminate between different transport pathways. However, quantitative estimates of the amounts of rubidium that could have entered the tubule cells from the lumen during the 20 and 30 second infusion periods indicate that luminal rubidium cannot be a major source. This follows not only from quantitative considerations of the amounts of rubidium filtered and those accumulating in cells (proximal tubule), but also from the rather long transit times of filtrate from the glomerulus to the distal convolution (30 to 70 sec). Rubidium uptake rates thus represent a means for evaluating differences in the overall potassium transport activity of individual tubule cells, largely those of the basolateral cell membrane.

Differences in rubidium uptake

The results obtained immediately after 20 or 30 seconds of rubidium administration demonstrate clearly that there are significant differences of rubidium uptake rates between the various cell types of the distal convolution. Tubule cells thought to be involved in sodium absorption—the distal convoluted tubule cells—and those mediating sodium absorption and potassium secretion—the connecting tubule and principal cells—exhibit high rates of rubidium uptake. In contrast, rubidium uptake into intercalated cells is comparatively low. Rubidium uptake into proximal convoluted tubule cells proceeds also at a significant rate, but is lower than in distal convoluted tubule, connecting tubule and principal cells.

The handling of rubidium by the distal tubule and the collecting duct is of interest. The marked differences between connecting tubule and principal cells on one hand, and intercalated cells on the other hand, support the view that transcellular potassium movement across the “late” distal tubule (a major

site of potassium secretion) proceeds preferentially through connecting tubule and principal cells. These cells are characterized by high contents of $\text{Na}^+\text{-K}^+\text{-ATPase}$ in the basolateral membrane and by significant sodium and potassium conductances in the apical cell membranes [31, 32]. In contrast, the comparatively-low rubidium uptake rates in intercalated cells are consistent with the view in that these cells do not participate in net sodium transport and potassium secretion [33], both processes that depend critically on basolateral $\text{Na}^+\text{-K}^+\text{-ATPase}$ activity. Intercalated cells have been found to have a very low $\text{Na}^+\text{-K}^+\text{-ATPase}$ content in the rat kidney [34] and are thought to play a significant role in either proton or bicarbonate secretion and in potassium reabsorption [3, 4], transport activities not directly linked to basolateral $\text{Na}^+\text{-K}^+\text{-exchange}$.

It is also noteworthy that the pattern of distribution of rubidium uptake along the nephron bears relationship to the $\text{Na}^+\text{-K}^+\text{-ATPase}$ activity in renal cortical tubules [35]. High levels of $\text{Na}^+\text{-K}^+\text{-ATPase}$ are localized in the proximal convoluted tubule, the thick ascending limb and the distal convoluted tubule, smaller $\text{Na}^+\text{-K}^+\text{-ATPase}$ activities have been observed in collecting duct cells [35, 36]. The relationship between $\text{Na}^+\text{-K}^+\text{-ATPase}$ content and rubidium uptake as measured in the present experiments is complicated by several factors: First, tubule $\text{Na}^+\text{-K}^+\text{-ATPase}$ content is usually referred to tubule length [35], a method that does not take into account cell thickness and protein content. In contrast, rubidium uptake in our studies is expressed as content per cell dry weight and unit time. For instance, protein content of proximal tubules is higher than that of the distal convolution [37]. These differences in protein content may account for the comparatively low rubidium uptake into proximal tubule cells. Second, in the present study rubidium uptake was measured in individual distal tubule cells, whereas $\text{Na}^+\text{-K}^+\text{-ATPase}$ is conventionally determined in tubule segments often consisting of cells with widely differing $\text{Na}^+\text{-K}^+\text{-ATPase}$ activities [34]. Both of these factors may explain the relatively-high rubidium uptake into principal cells compared to that of the proximal tubule.

Taken together, the correlation between rubidium uptake and $\text{Na}^+\text{-K}^+\text{-ATPase}$ activity suggests that the basolateral $\text{Na}^+\text{-K}^+\text{-ATPase}$ activity is one of the key factors contributing to the rate at which rubidium ions are taken up into renal tubule cells. However, many observations in tubule cells have shown close functional coupling between the rate of active $\text{Na}^+\text{-K}^+\text{-exchange}$ and the passive potassium permeability of the apical [33] and basolateral cell membrane [38–40] of tubule cells. Inasmuch as active pump rate regulates the potassium permeability, both of these factors will ultimately determine the rate of rubidium uptake. The possible participation of potassium chloride cotransport in rubidium uptake is presently unknown.

Another functional correlation deserves comment. The cell rubidium contents determined immediately after rubidium injection decrease significantly as one proceeds from the beginning of the surface distal tubule, that is, the distal convoluted tubule (the "early" distal tubule), to the connecting tubule and to the beginning segment of the cortical collecting duct (the "late" distal tubule). The finding that the highest rubidium uptake rates were observed in distal convoluted tubule cells, followed by the connecting tubule cells and the principal cells shows a remarkable parallelism to the sodium load presented to

successive segments of the distal convolution and to the rate of sodium transport [41].

After terminating the rubidium injection, a steep decline in plasma rubidium concentration was observed, followed with some time delay by a more gradual fall in cell rubidium content. These events led the cell/plasma rubidium gradient eventually to surpass the corresponding cell/plasma gradient of potassium. Thus, after 420 seconds the following rubidium/potassium cell/plasma ratios were observed: proximal convoluted tubule cell, 6.5; distal convoluted tubule cell, 3.9; connecting tubule cell, 3.9; principal cell, 3.3; intercalated cell, 3.0. Values above unity indicate that rubidium is relatively more concentrated in some tubule cell than potassium. The maintenance of a higher intrato-extracellular concentration gradient for rubidium compared to potassium has also been observed under steady-state conditions by us (unpublished observations) and other investigators [42]. The preferential cellular retention of rubidium compared to that of potassium in our experiments could be explained by either higher active uptake of rubidium into the cells via primary or secondary active transport mechanisms (that is, basolateral ATPase-mediated sodium-potassium exchange or potassium chloride cotransport [43]), by restricted exit (low rubidium permeability) from cell to the extracellular fluid, and/or rapid disappearance of rubidium from the extracellular fluid. The latter factor may be an important one, because plasma rubidium levels rapidly declined after the bolus injection. Our data do not allow us to discriminate between these possible factors. However, higher active uptake of rubidium compared to potassium seems unlikely, since the potency of rubidium for activating the $\text{Na}^+\text{-K}^+\text{-ATPase}$ is only slightly less than that of potassium [26]. On the other hand, certain potassium-selective channels in epithelial cells discriminate between potassium and rubidium allowing the passage of rubidium to only a restricted extent [29, 30]. Functional cell heterogeneity of rubidium retention was also observed. At equally low rubidium concentrations for all cells in the extracellular fluid proximal tubule cells retained rubidium more than those of the distal convolution. The rubidium retention observed by us and others [42] is consistent with active (pump-mediated) rubidium uptake and, compared with potassium, delayed exit of rubidium from tubule cells into the extracellular fluid.

Alterations in distal sodium and potassium transport

When large quantities of sodium chloride are administered intravenously distal sodium delivery and, as a consequence, active sodium reabsorption along the surface distal tubule are markedly stimulated. Thus, the present protocol of infusing hypertonic sodium chloride has been shown to result not only in elevated sodium concentrations of the tubule fluid along the total length of the surface distal tubule but also in sharply increased rates of sodium reabsorption and potassium secretion along the distal convolution [12, 13]. If indeed a substantial component of rubidium influx into tubule cells is due to uptake via the $\text{Na}^+\text{-K}^+\text{-ATPase}$ pathways, alterations in distal sodium and potassium transport would be expected to induce corresponding changes of rubidium uptake into the cells involved in these transport operations.

The present study supports this thesis and provides information about the cell types and the cellular mechanisms responsible for the rise in sodium transport during increased distal

sodium delivery: only distal convoluted tubule, connecting tubule and principal cells, but not intercalated cells, showed a marked stimulation of rubidium uptake. Rubidium uptake in proximal tubule cells was also not significantly affected by the administration of hypertonic sodium chloride, a finding consistent with no marked changes in sodium reabsorption in these conditions [44]. The observations of rubidium uptake into cells of the distal convolution are in accord not only with the observed transport studies referred to above, but also with the recent finding that an acute increase in distal fluid sodium chloride concentrations is accompanied by a rise in cell sodium concentrations of all but the intercalated cells [45]. Thus, it may be concluded that increased distal fluid sodium concentrations lead to enhanced sodium entry across the luminal membrane of the sodium transporting cells. This causes a rise in cell sodium concentrations and, as a consequence, a stimulation of active sodium extrusion and potassium (rubidium) uptake via the Na^+/K^+ -ATPase.

Acknowledgments

Parts of this work were published in abstract form in *Proc Int Cong Physiol Sci* 16:419, 1986 and in *Kidney Int* 1988 (in press). G. Giebisch was supported by the Alexander von Humboldt-Stiftung. Work in the authors laboratories was supported by grants from the Deutsche Forschungsgemeinschaft (Be 963/2-2) and the NIH grant 17433. The technical assistance of M. Schramm, P. Jauernig, and I. Öztürk is gratefully acknowledged.

Reprint requests to Dr. Franz X. Beck, Physiologisches Institut der Universität, Pettenkoferstraße 12, D-8000 München 2, Federal Republic of Germany.

References

1. CRAYEN M, THOENES W: Architektur und cytologische Charakterisierung des distalen Tubulus der Rattenniere. *Fortschr Zool* 23: 279-288, 1975
2. STANTON BA, BIEMESDERFER D, WADE JB, GIEBISCH G: Structural and functional study of the rat distal nephron: Effects of potassium adaptation and depletion. *Kidney Int* 19:36-48, 1981
3. GIEBISCH G, MALNIC G, BERLINER RW: Renal transport and control of potassium excretion, chapter 6, in *The Kidney* (3rd ed), edited by BRENNER BM, Rector FC Jr, Philadelphia, WB Saunders, 1986, pp. 177-205
4. KOEPPEN B, GIEBISCH G, MALNIC G: Mechanism and regulation of renal tubular acidification, chapter 65, in *The Kidney—Physiology and Pathophysiology*, edited by SELDIN DW, GIEBISCH G, New York, Raven Press, 1985 (vol 2), pp. 1491-1525
5. BECK F, BAUER R, BAUER U, MASON J, DÖRGE A, RICK R, THURAU K: Electron microprobe analysis of intracellular elements in the rat kidney. *Kidney Int* 17:756-763, 1980
6. BECK F, DÖRGE A, MASON J, RICK R, THURAU K: Element concentrations of renal and hepatic cells under potassium depletion. *Kidney Int* 22:250-256, 1982
7. RELMAN AS: The physiological behavior of rubidium and cesium in relation to that of potassium. *Yale J Biol Med* 29:248-262, 1956
8. USSING HH, KRUFFER P, HESS THAYSEN J, THORN NS: The alkali metal ions in biology, in *Handbuch der experimentellen Pharmakologie*, edited by EICHLER O, FARAH A, Berlin, Springer-Verlag, 1960, Band 13, pp. 114-129
9. RELMAN AS, ROY AM, SCHWARTZ WB: The acidifying effect of rubidium in normal and potassium-deficient alkalotic rats. *J Clin Invest* 34:538-544, 1955
10. KUNIN AS, DEARBORN EH, BURROWS BA, RELMAN AS: Comparison of renal excretion of rubidium and potassium. *Am J Physiol* 197:1297-1302, 1959
11. SCHAFFER JA, TROUTMAN SL: Effect of ADH on rubidium transport in isolated perfused rat cortical collecting tubules. *Am J Physiol* 250:F1063-F1072, 1986
12. KHURI RN, WIEDERHOLT M, STRIEDER N, GIEBISCH G: Effects of flow rate and potassium intake on distal tubular potassium transfer. *Am J Physiol* 228:1249-1261, 1975
13. KHURI RN, WIEDERHOLT M, STRIEDER N, GIEBISCH G: Effects of graded solute diuresis on renal tubular sodium transport in the rat. *Am J Physiol* 228:1262-1268, 1975
14. KRIZ W, KAISLING B: Structural organization of the mammalian kidney, (chapter 14) in *The Kidney—Physiology and Pathophysiology*, edited by SELDIN DW, GIEBISCH G, New York, Raven Press, 1985, pp. 265-306
15. JAMISON RL, KRIZ W: *Urinary concentrating mechanism: Structure and function*. New York, Oxford University Press, 1982, p. 293
16. DÖRGE A, RICK R, GEHRING K, THURAU K: Preparation of freeze-dried cryosections for quantitative X-ray microanalysis of electrolytes in biological soft tissues. *Pflügers Arch* 373:85-97, 1978
17. BAUER R, RICK R: Computer analysis of X-ray spectra (EDS) from thin biological specimens. *X-Ray Spectrom* 7:63-69, 1978
18. HALL TA: The microprobe assay of chemical elements, in *Physical Techniques in Biological Research* (2nd ed), edited by OSTER G, New York, Academic Press, 1971, pp. 157-275
19. FÜHR J, KACZMARCZYK J, KRÜTTGEN CD: Eine einfache colorimetrische Methode zur Inulinbestimmung für Nieren-Clearance-Untersuchungen bei Stoffwechselfgesunden und Diabetikern. *KlinWochenschr* 33:729-730, 1955
20. DIXON WJ: *BMDP Statistical Software*. Berkeley, Los Angeles, London, University of California Press, 1985
21. BURCH GE, THREEFOOT SA, RAY CT: The rate of disappearance of Rb^{86} from the plasma, the biologic decay rates of Rb^{86} , and the applicability of Rb^{86} as a tracer of potassium in man with and without chronic congestive heart failure. *J Lab Clin Med* 45:371-394, 1955
22. MOREL F: Les modalités de l'excrétion du potassium par le rein: étude expérimentale à l'aide du radio-potassium chez le lapin. *Helv Physiol Acta* 13:276-294, 1955
23. WORK J, TROUTMAN SL, SCHAFFER JA: Transport of potassium in the rabbit pars recta. *Am J Physiol* 242:F226-F237, 1982
24. SCHAFFER JA, TROUTMAN SL: Potassium transport in cortical collecting tubules from mineralocorticoid-treated rat. *Am J Physiol* 253:F76-F88, 1987
25. WARDEN DH, SCHUSTER VL, STOKES JB: Comparison of Rb and K transport in the rabbit cortical collecting tubule (CCT). *Kidney Int* 31:443, 1987
26. SKOU JC: Enzymatic basis for active transport of Na^+ and K^+ across cell membrane. *Physiol Rev* 45:596-617, 1965
27. AITON JF, BROWN CDA, OGDEN P, SIMMONS NL: K^+ transport in 'tight' epithelial monolayers of MDCK cells. *J Membr Biol* 65:99-109, 1982
28. KNAUF PA: Anion transport in erythrocytes, chapter 12, in *Physiology of membrane disorders*, edited by ANDREOLI TE, HOFFMAN JF, FANESTIL DD, SCHULTZ SG: (2nd ed), New York, London, Plenum Medical Book Company, 1986, pp. 191-220
29. DAWSON CM, CROGHAN PC, SCOTT AM, BANGHAM JA: Potassium and rubidium permeability and potassium conductance of the beta-cell membrane in mouse islets of Langerhans. *Q J Exp Physiol* 71:205-222, 1986
30. GALLACHER DV, MARUYAMA Y, PETERSEN OH: Patch-clamp study of rubidium and potassium conductances in single cation channels from mammalian exocrine acini. *Pflügers Arch* 401:361-367, 1984
31. KOEPPEN BM, BIAGI BA, GIEBISCH GH: Intracellular microelectrode characterization of the rabbit cortical collecting duct. *Am J Physiol* 244:F35-F47, 1983
32. O'NEIL RG, SANSOM SC: Characterization of apical cell membrane Na^+ and K^+ conductances of cortical collecting duct using microelectrode techniques. *Am J Physiol* 247:F14-F24, 1984
33. MUTO S, GIEBISCH G, SANSOM S: Effects of adrenalectomy on CCD: Evidence for differential response of two cell types. *Am J Physiol* 253:F742-F752, 1987
34. KASHGARIAN M, BIEMESDERFER D, CAPLAN M, FORBUSH B III: Monoclonal antibody to Na, K -ATPase: Immunocytochemical localization along nephron segments. *Kidney Int* 28:899-913, 1985

35. KATZ AI: Distribution and function of classes of ATPases along the nephron. *Kidney Int* 29:21–31, 1986
36. GARG LC, KNEPPER MA, BURG MB: Mineralocorticoid effects on Na,K-ATPase in individual nephron segments. *Am J Physiol* 240:F536–F544, 1981
37. EL MERNISSI G, CHABARDÈS D, DOUCET A, HUS-CITHAREL A, IMBERT-TEBOUL M, LE BOUFFANT F, MONTÉGUT M, SIAUME S, MOREL F: Changes in tubular basolateral membrane markers after chronic DOCA treatment. *Am J Physiol* 245:F100–F109, 1983
38. COHEN B, GIEBISCH G: Relationship between potassium conductance and transport in renal tubular epithelium, in *Information and Energy Transduction in Biological Membranes*, edited by HELMREICH EJM, PASSOW H, New York, Alan Liss, 1984, pp. 391–401
39. LAU KR, HUDSON RL, SCHULTZ SG: Cell swelling increases a barium-inhibitable, potassium conductance in the basolateral membrane of *Necturus* small intestine. *Proc Natl Acad Sci USA* 81:3591–3594, 1984
40. MATSUMURA Y, COHEN B, GUGGINO WB, GIEBISCH G: Regulation of the basolateral potassium conductance of the *Necturus* proximal tubule. *J Membr Biol* 79:153–161, 1984
41. GIEBISCH G, WINDHAGER EE: Renal tubular transfer of sodium chloride and potassium. *Am J Med* 36:643–669, 1964
42. KILPATRICK R, RENSCHLER HE, MUNRO DS, WILSON GM: A comparison of the distribution of ^{42}K and ^{86}Rb in rabbit and man. *J Physiol* 133:194–201, 1956
43. ELLISON DH, VELAZQUEZ H, WRIGHT FS: Stimulation of distal potassium secretion by low lumen chloride in the presence of barium. *Am J Physiol* 248:F638–F649, 1985
44. GIEBISCH G, KLOSE RM, WINDHAGER EE: Micropuncture study of hypertonic sodium chloride loading in the rat. *Am J Physiol* 206:687–693, 1964
45. BECK F, DÖRGE A, RICK R, SCHRAMM M, THURAU K: The distribution of potassium, sodium and chloride across the apical membrane of renal tubule cells: Effect of acute metabolic alkalosis. *Pflügers Arch* (in press)